

Fractal scaling of small-angle neutron scattering from nonionic micellar solutions below the cloud temperature

S. V. G. Menon,¹ P. S. Goyal,² B. A. Dasannacharya,² and P. Thiyagarajan³

¹Theoretical Physics Division, Bhabha Atomic Research Centre, Bombay 400 085, India

²Solid State Physics Division, Bhabha Atomic Research Centre, Bombay 400 085, India

³Intense Pulsed Neutron Source, Argonne National Laboratory, Argonne, Illinois 60439

(Received 11 July 1995)

Power-law variations of small-angle neutron-scattering intensities from nonionic micellar solutions of isooctylphenoxy polyethoxy ethanol (Triton X-100) in D₂O for a range of concentrations (1–4 wt %) and temperatures (295–335 K) are interpreted in terms of simple models of fractal aggregates. The results show a large increase in dimensionality from ~ 1 at ambient temperature to ~ 2.3 near the cloud points. The variation of fractal dimension with temperature is almost the same for the three concentrations studied. Thus one arrives at a picture of micellar aggregates becoming more and more tenuous as cloud points are approached. [S1063-651X(96)08305-5]

PACS number(s): 82.70–y, 05.40+j, 64.70.–p, 61.10.Eq

An exhaustive set of small-angle neutron-scattering (SANS) experiments from Triton X-100 (isooctylphenoxy polyethoxy ethanol, Aldrich) solutions in D₂O covering a wide range of concentrations (1–15 wt %) and temperatures (295–335 K) was reported by us recently [1]. These solutions show the well-known clouding phenomena [2] with a lower consolute point in the phase diagram at $\phi_c \sim 6$ wt % and temperature $T_c \sim 335$ K. The clouding temperatures for 1, 2, 4, 8, 12, and 15 wt % solutions, the systems for which SANS measurements were made, are 336.5, 336, 335, 335.5, 337, and 338 K, respectively. The measurements were made at the Intense Pulsed Neutron Source at Argonne National Laboratory, Argonne, Illinois, U.S.A., by using the small-angle diffractometer (SAD) [3].

SANS intensities in these experiments, especially for low scattering vector $Q (< 0.03 \text{ \AA}^{-1})$, show a significant increase (see Figs. 1–3) as the temperature approaches the cloud points [1]. For instance, in the case of 4 wt % solution the intensity at $Q \sim 0.006 \text{ \AA}^{-1}$ increases by one order of magnitude as the solution temperature changes from 295 to 335.5 K. Baxter's sticky hard sphere model [4] was used to compute the intermicellar structure factor for interpreting the temperature variation of SANS intensities; micelles were modeled as oblate ellipsoids of revolution. This model depicts micelles as particles interacting via a short ranged (temperature dependent) attractive potential [5,6] which is responsible for the clouding behavior. The temperature dependent potential depth U_0 , embedded in Baxter's stickiness parameter τ , was the only adjustable parameter in this analysis. For solutions with $\phi > \phi_c$, the model provided a good fit. A linear variation of the potential depth — with a value around $3K_B T_c$ at the lower consolute point — was deduced from these analyses [1].

For lower Triton X-100 concentrations, i.e., ($\phi < \phi_c$), the model was quite inadequate to explain the data. For example, in the case of 1 wt % data, the model failed to show any temperature variation of SANS intensity for $T > 313$ K (see Fig. 1) whereas the experimental results indicated a threefold increase at $T \sim 331$ K (for $Q \sim 0.006 \text{ \AA}^{-1}$) in comparison to

the data at 313 K. This is not very surprising since micelles, which have an aggregation number ~ 145 and an effective diameter of 75 \AA [1], are at a mean separation of 250 \AA in the 1 wt % solution. The short ranged interactions incorporated in Baxter's model are therefore totally ineffective to induce particle clustering needed to produce the buildup of scattering intensities. Use of more detailed intermicellar potentials [7], liquid state theories, and polydispersity in micellar size did not improve the results. These approaches assume that density fluctuations [2,8–10] alone can account for the buildup of scattering intensity. However, for Triton X-100 surfactant — which has 14 carbon atoms in the hydrophobic part and an average of ten ethylene oxide units in the hydrophilic chain — there is a possibility of micellar growth [2,11–14] on increase of temperature. While growth of micelles and critical fluctuations can be mixed together in principle in data analysis, their separation would be quite arbitrary. Therefore a simple alternate approach is necessary to characterize the SANS data for $\phi < \phi_c$.

We noticed that SANS intensities $I(Q)$ in this regime show a power-law variation (see Figs. 2 and 3) with respect to Q for $Q < 0.03 \text{ \AA}^{-1}$; for higher values of Q they are determined by the micellar form factor. In this paper, we report the exponents (D) extracted from the power-law variations, $I(Q) \sim Q^{-D}$, with the use of simple models of structure factor of fractal aggregates and arrive at new conclusions regarding variation of D as the cloud point is approached. It is known that correlated regions in several binary mixtures near their critical points have a fractal structure [15]. Therefore it is plausible that the structure of micellar aggregates — whether they arise out of growth or density fluctuations — can be modeled with fractal concepts. For the sake of completeness, we first recall the scattering functions used in the analysis.

For monodisperse individual scatterers, of number density n , the SANS intensity can be factored as [16]

$$I(Q) = n \langle |F(Q)|^2 \rangle \bar{S}(Q), \quad (1)$$

where $F(Q)$ is the single particle scattering function

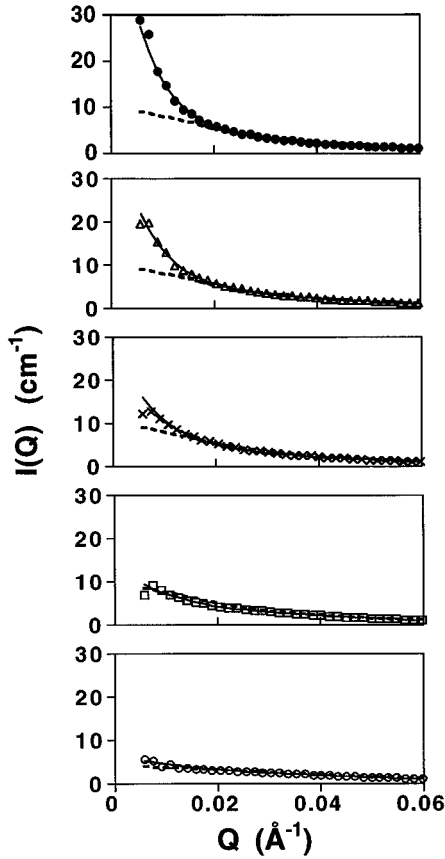


FIG. 1. The absolute differential scattering cross section of 1 wt % Triton X-100 solution in D_2O at 295 K (o), 313 K (\square), 323 K (\times), 328 K (\triangle), and 331 K (\bullet) in the Q region $\leq 0.06 \text{ \AA}^{-1}$. Between the fractal model (—) and Baxter's model (---), the former fits the data well in the whole Q region, while the latter fails in the low Q region.

$$F(Q) = \int_{v_p} [\rho(\mathbf{r}) - \rho_s] \exp(i\mathbf{Q} \cdot \mathbf{r}) d\mathbf{r}. \quad (2)$$

Here, $\rho(\mathbf{r})$ and ρ_s are, respectively, the scattering length densities of the particle and solvent, and v_p is the particle volume. The angular brackets in Eq. (1) indicate averages over all particle orientations. The effective structure factor $\bar{S}(Q)$ for an isotropic system can be expressed as [17]

$$\bar{S}(Q) = 1 + \frac{\langle |F(Q)|^2 \rangle}{\langle |F(Q)|^2 \rangle} [S(Q) - 1], \quad (3)$$

where $S(Q)$ describes the center-of-mass correlations. The prefactor $\langle |F|^2 \rangle / \langle |F|^2 \rangle$ accounts for the orientation distribution of particles. For the present application, this approximation to $\bar{S}(Q)$ is adequate since the axial ratio of the ellipsoidal micelle is around 2 [17]. The variation of the above prefactor because of the distribution in sizes and shapes, if any, has been neglected. A generalization of the Ornstein-Zernike formula for the center-of-mass structure factor is [18]

$$S(Q) = 1 + \frac{(S_0 - 1)}{(1 + Q^2 \xi^2)^{D/2}}. \quad (4)$$

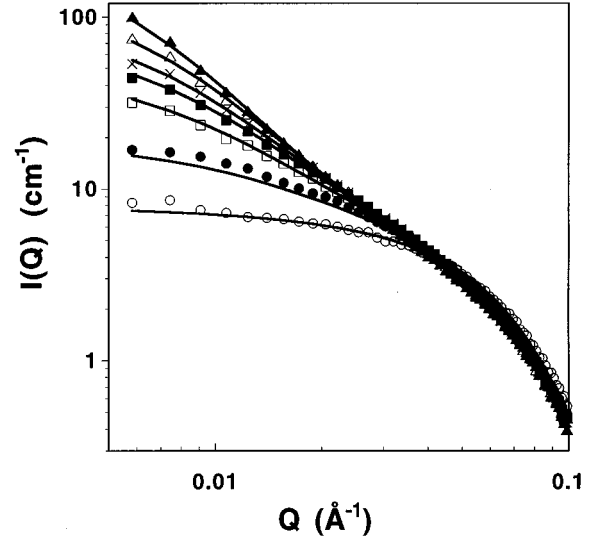


FIG. 2. The absolute differential scattering cross section of 2 wt % Triton X-100 solution in D_2O at 295 K (o), 313 K (\bullet), 323 K (\square), 328 K (\blacksquare), 330 K (\times), 332 K (\triangle), 334 K (\blacktriangle). The solid lines are fits with the fractal model. Note that the data merge at $Q > 0.03 \text{ \AA}^{-1}$ for all temperatures.

Here, D is the dimensionality of the structure of the scattering units, S_0 is the compressibility factor, and ξ is the correlation length. Equations (1)–(4) together with a model for the micelle form factor can be used to extract the dimensionality D . An alternate formula that can be used is the structure factor for a fractal aggregate discussed in several papers [19–22]:

$$S(Q) = 1 + A \left[\frac{\xi}{r_0} \right]^D \frac{\Gamma(D+1)}{(1 + Q^2 \xi^2)^{(D-1)/2}} \times \frac{\sin[(D-1) \arctan(Q\xi)]}{(D-1)Q\xi}. \quad (5)$$

The constant $A \sim 1$ is an amplitude parameter [20,23] which describes the packing of particles (of radius $r_0 = 37.5 \text{ \AA}$), the fractal D is the dimensionality of an average aggregate, ξ is an exponential decay length [20,23] introduced to describe finite clusters, and $\Gamma(x)$ is the gamma function. ξ is related to the radius R of the average aggregate as $R = \xi[(D+1)(D+2)/2]^{1/2}$ [23]. That is, ξ has a similar meaning in Eqs. (4) and (5). Both Eqs. (4) and (5) yield a power-law variation $S(Q) \sim Q^{-D}$ for $Q \gg \xi^{-1}$; they reduce to the Guinier form for $Q \ll \xi^{-1}$. Extended regular objects also yield power-law decay in SANS intensity. In the absence of *a priori* knowledge about their dimensionality, a first approximation would be to assume that they are also covered in this formulation. For example, a long cylindrical aggregate can be constructed out of small cylindrical units or a tortuous two-dimensional sheet can be built up with a disc as the unit.

Modeling of scattering profiles over a limited Q range alone cannot provide an unambiguous picture of micellar structure, let alone settle the issue of critical fluctuations and/or micellar growth. Use of Eq. (1) which factors the scattering intensity into $P(Q) (= \langle |F(Q)|^2 \rangle)$ and $\bar{S}(Q)$ in situations where both aspects are likely to be present — as in

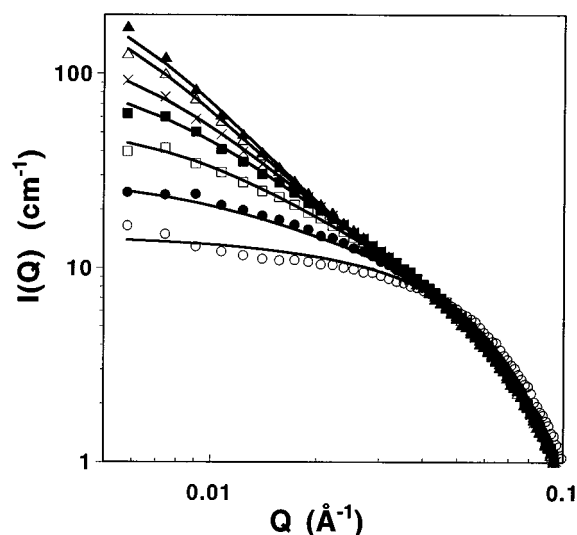


FIG. 3. The absolute differential scattering cross section of 4 wt % Triton X-100 solution in D_2O at 295 K (o), 313 K (●), 323 K (□), 328 K (■), 330 K (×), 332 K (△), 334 K (▲). The solid lines are fits with the fractal model. The behavior is similar to that for 2 wt % solution.

Triton X-100 solutions — is only a first approximation. The minimal set of parameters [ξ , S_0 , and D in Eq. (4) and A , ξ , and D in Eq. (5)] extracted from the data are hoped to provide the shape and extent of an average aggregate. In particular, the variation of D with temperature can yield some insight into the evolution of solution structure, as we will see later.

The basic unit used to build the fractal structure has been assumed to be an oblate micelle. The detailed structure and form factor $P(Q)$ of this unit was obtained from 1 wt % SANS data at 295 K and is given in the earlier paper [1]. For the sake of completeness we recall that Triton X-100 micelles can be modeled as a double shell oblate ellipsoid of revolution. The inner core with axes 20 and 70 Å contains the hydrophobic segments of the surfactant. The outer shells of hydrophilic segments have axes 45 and 95 Å. The aggregation number is around 145 and there are about 20 water molecules per surfactant molecule in the outer shell. This model of Triton X-100 is consistent with available results from light scattering, x-ray, and NMR studies [24–26].

The measured SANS intensities (or cross sections) together with the fits using the formulas discussed earlier are shown in Figs. 1–3 for 1, 2, and 4 wt % solutions, respectively. Both models of $S(Q)$ gave quite comparable results, the solid lines in the figures are based on Eq. (5). For clarity of presentation and comparison with the results of Baxter's model (dashed line), data for $Q < 0.06 \text{ \AA}^{-1}$ only are shown in Fig. 1. In spite of their simplicity, the structure factor models of fractals provide excellent agreement. This is further elaborated in Figs. 2 and 3 where data from 2 and 4 wt % solution for seven temperatures are presented in logarithmic scales. For the three concentrations, the parameter ξ varied from 100 to 300 Å as temperature approached the cloud points. These values must be taken as lower bounds of correlation lengths since the power-law variation extends up

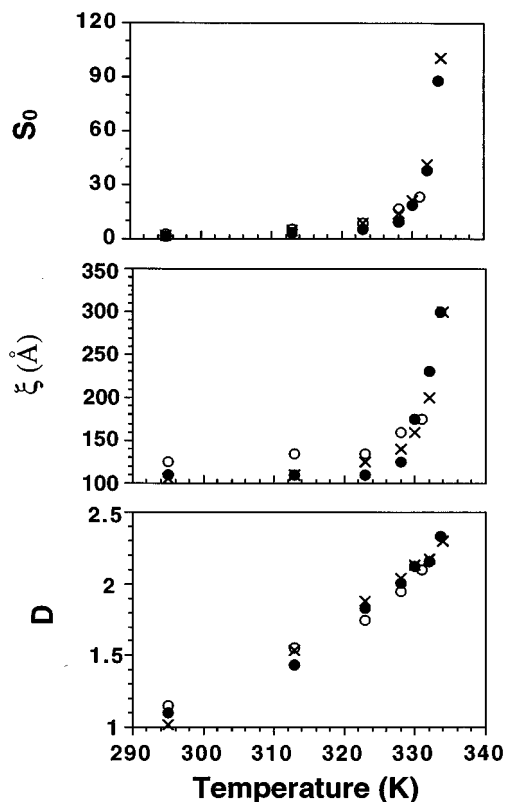


FIG. 4. Temperature dependence of fractal dimension (D), correlation length (ξ), and the compressibility factor S_0 derived from fractal model fits for Triton X-100 solution in D_2O at 1 wt % (o), 2 wt % (●), and 4 wt % (×).

to the smallest $Q \sim 0.006 \text{ \AA}^{-1}$ in the data. The compressibility factor, S_0 in Eq. (4), increased from ~ 2 at room temperature to ~ 100 near cloud points. The amplitude parameter A — when Eq. (5) was used — remained nearly constant in the range 0.4 – 0.5 except for the lowest temperature (295 K), where it was in the range 0.2–0.3. Both models of $S(Q)$ showed that D increases from a value close to 1 ± 0.15 at low temperature to around 2.3 ± 0.1 at the highest temperature. Within experimental errors, the temperature dependence of ξ , S_0 , and D is the same for the three concentrations, as seen in Fig. 4. Thus we find that the solution structure remains more or less the same for concentrations $\phi < \phi_c$. Micellar aggregates, which have a linear structure at room temperature (fractal dimension $D \sim 1$), are found to become more and more tenuous as temperature is increased. These findings together with the micellar model we have used suggest that an average aggregate would be like a strip of a ribbon (of thickness $\sim 45 \text{ \AA}$) at room temperature. The aggregates extend in both dimensions and become a tortuous object near cloud points. It is interesting to note that this behavior of the solution is independent of the surfactant concentration.

Some of the earlier investigations on micellar solutions have given evidence of fractal structure [19,27,28]. We also note that there exist growth models wherein a parameter can be tuned to generate random fractals of a specified dimension [29]. While these applications use fractal concepts to model

purely interparticle correlations, the present work shows their usefulness in characterizing more complicated structures resulting out of growth and critical fluctuations.

A few conclusions emerge from this SANS study of Triton X-100 solutions: (i) models of structure factor of fractal aggregates provide a simple way to characterize the solution structure near the cloud points; (ii) the nature of the aggregates, more or less, remains the same for concentrations $\phi < \phi_c$, in particular, the variation of ξ , S_0 , and D with temperature is the same for the three concentrations; and (iii)

it would be worthwhile to extend the measurements to lower Q values so that the correlation lengths can be determined accurately.

We thank S. L. Narasimhan for bringing some of the references to our attention and many fruitful discussions. This work benefited from the use of the Intense Pulsed Neutron Source at Argonne National Laboratory which is funded by the United States Department of Energy, BES – Material Science, under Contract No. W-31-109-ENG-38.

-
- [1] P. S. Goyal, S. V. G. Menon, B. A. Dasannacharya, and P. Thiyagarajan, *Phys. Rev. E* **51**, 2308 (1995).
- [2] V. Degiorgio, in *Physics of Amphiphiles: Micelles, Vesicles and Microemulsions*, edited by V. Degiorgio and M. Corti (North-Holland, Amsterdam, 1985).
- [3] J. E. Epperson, J. M. Carpenter, R. K. Crawford, P. Thiyagarajan, T. E. Klippert, and D. G. Wozniak (unpublished).
- [4] R. J. Baxter, *J. Chem. Phys.* **49**, 2770 (1968).
- [5] J. B. Hayter and M. Zulauf, *Colloid Polym. Sci.* **260**, 1023 (1982).
- [6] J. N. Israelachvili, *Intermolecular and Surface Forces* (Academic Press, New York, 1992).
- [7] L. Reatto, in *Surfactants in Solution*, edited by K. L. Mittal (Plenum, New York, 1989), Vol. 7.
- [8] M. Corti, C. Minero, and V. Degiorgio, *J. Phys. Chem.* **88**, 309 (1984).
- [9] M. Corti and V. Degiorgio, *Phys. Rev. Lett.* **55**, 2005 (1985).
- [10] L. J. Magid, R. Trilo, and S. S. Johnson, *J. Phys. Chem.* **88**, 5730 (1984).
- [11] B. Lindman and H. Wennerstrom, *J. Phys. Chem.* **95**, 6053 (1991).
- [12] T. R. Carle and D. Blankschtein, *J. Phys. Chem.* **96**, 459 (1992).
- [13] C. B. Douglas and E. W. Kaler, *Langmuir* **10**, 1075 (1994).
- [14] R. Trilo, L. J. Magid, J. S. Johnson, and H. R. Child, *J. Phys. Chem.* **86**, 3689 (1982).
- [15] D. Beysens, P. Guenoun, and F. Perrot, *J. Phys. Condens. Matter* **2**, 127 (1990).
- [16] S. H. Chen and T. L. Lin, in *Methods of Experimental Physics* (Academic Press, New York, 1987), Vol. 23B, p. 489.
- [17] M. Kotlarchyk and S. H. Chen, *J. Chem. Phys.* **79**, 2461 (1983).
- [18] M. E. Fisher and R. J. Burford, *Phys. Rev.* **156**, 583 (1967).
- [19] S. H. Chen and J. Teixeira, *Phys. Rev. Lett.* **57**, 2583 (1986).
- [20] T. Freltoft, J. K. Kjems, and S. K. Sinha, *Phys. Rev. B* **33**, 269 (1986).
- [21] P. Dimon, S. K. Sinha, D. A. Weitz, C. R. Safinya, G. S. Smith, W. A. Varady, and H. M. Lindsay, *Phys. Rev. Lett.* **57**, 595 (1986).
- [22] P. W. Schmidt, *J. Appl. Crystallogr.* **24**, 414 (1991).
- [23] Z. Yanovei and S. Meriani, *J. Appl. Crystallogr.* **27**, 782 (1994).
- [24] R. J. Robson and E. A. Dennis, *J. Phys. Chem.* **81**, 1075 (1977).
- [25] N. Stubicar, J. Matejas, P. Zipper, and R. Wilfing, in *Surfactants in Solution*, edited by K. L. Mittal (Plenum, New York, 1989), Vol. 7, p. 181.
- [26] W. Brown, R. Rydman, J. V. Stam, M. Almgren, and G. Svensk, *J. Phys. Chem.* **93**, 2512 (1989).
- [27] S. H. Chen, J. Rouch, F. Sciortino, and P. Tartaglia, *J. Phys. Condens. Matter* **6**, 10855 (1994).
- [28] E. Ducros, S. Haouache, R. Rouch, K. Hamano, K. Fukuhara, and P. Tartaglia, *Phys. Rev. E* **50**, 1291 (1994).
- [29] P. Meakin, F. Leyvraz, and H. E. Stanley, *Phys. Rev. A* **31**, 1195 (1985).